Unique Aerial Photographs of Eddy Circulations in Marine Stratocumulus Clouds

Bradley M. Muller, Christopher G. Herbster, and Frederick R. Mosher

Department of Applied Aviation Sciences

Embry-Riddle Aeronautical University, Daytona Beach, Florida

Submitted to *Monthly Weather Review* October, 2013

Corresponding author address:

Dr. Bradley M. Muller

Dept. of Applied Aviation Sciences

Embry-Riddle Aeronautical University

600 S. Clyde Morris Blvd.

Daytona Beach, FL 32114-3900

E-mail: mullerb@erau.edu

Abstract

Aerial photographs of cyclonic, von Karman-like vortices in the marine stratocumulus clouds off the California coast, taken by a commercial pilot near Santa Cruz Island and Grover Beach, are presented. It is believed that these are the first photographs of such eddies taken from an airplane, to appear in publication.

Both eddies occurred with strong inversions above a shallow marine boundary layer, in the lee of high, inversion-penetrating terrain. Tower and surface wind measurements demonstrate that the Grover Beach eddy was not just a cloud-level feature, but extended through the marine atmospheric boundary layer (MABL) to the surface. 2-3C^{o} temperature increases and then decreases with the eddy passage suggest cross-inversion mixing of warm, dry air into the MABL, producing a cloud-free, warm-core "eye." Additionally, the sequence of wind reversals and temperature rises and falls from different levels of the tower suggest that the eddy is leaning forward as it passes the tower. Satellite-tracked eddy motions also suggest cross-inversion mixing: the eddy first moved toward the southwest, consistent with the northeasterly inversion-layer winds, but ultimately turned toward the east, apparently embedded in the westerly MABL flow rounding San Luis point. While it is not possible to unambiguously determine the eddy formation mechanism from the available data, observed characteristics were consistent with hypotheses from the theoretical literature on low Froude number, continuously stratified flow over obstacles involving tilting of baroclinically-generated "backward-rolling" (negative) horizontal vorticity into a vertical orientation by differential vertical motion in the lee of the high terrain.

1. Introduction

On July 16, 2006, and again on September 12, 2006, a pilot flying California coastal routes for SkyWest Airlines observed and photographed cyclonic vortices in marine stratocumulus clouds just off the coast (Capt. Peter Weiss, personal communication). The first (July 16) occurred on the north side of Santa Cruz Island (Figure 1) within what appeared from satellite imagery to be the southeasterly flow portion of a larger Catalina eddy circulation. The second (September 12) was spotted off Grover Beach downwind of a coastal headland (Fig. 2) southwest of San Luis Obispo, within a generally northwesterly marine atmospheric boundary layer (MABL) flow regime. Based on estimates from GOES satellite imagery, these eddy circulations in the clouds appeared to be on the order of 10-25 kilometers in diameter, placing them on the borderline between the meso-gamma and meso-beta scales of phenomena (2-20 km and 20-200 km, respectively, Orlanski 1975). Each contained a round cloud-free “eye” or hole of 2-3 kilometers diameter at their center.

Casual inspection of GOES satellite imagery of the West Coast region of North America reveals that similar eddies in the stratocumulus-topped MABL, on the order of tens of kilometers, are a relatively common occurrence near peninsulas, headlands, and downwind of islands. Many investigators have likened these relatively small-scale circulations, and similar features in other parts of the world, to von Karman vortices (Hubert and Krueger 1962; Chopra and Hubert 1965, Lyons and Fujita 1968; Thomson et al. 1977; Ruscher and Deardorff 1982; Etling 1989; Young and Zawislak 2006).

A number of meso-beta scale (20-200 km) eddies appear on a regular basis in the near-shore marine environment and have been described in the literature. They include the Catalina eddy (e.g. Rosenthal 1968; Bosart 1983; Wakimoto 1987; Mass and Albright 1989; Eddington et al.1992; Thompson et al. 1997; Parish et al. 2013), the Gaviota and midchannel eddies (Kessler and Douglas 1991; Douglas and Kessler 1991; Hanna et al. 1991; Wilczak et al. 1991; Dorman and Winant 2000), the Santa Cruz Eddy (Archer et al. 2005; Archer and Jacobson 2005), and the Antalya Cyclone (Alpert et al. 1999). Eddies at this scale are important because they are persistent and large enough to influence local stratus cloud formation, air quality, and surface wind fields in coastal regions (Wakimoto 1987; Hanna et al. 1991; Archer et al. 2005). The preceding modeling and observational studies indicate that these eddies result from complex interactions between a strong boundary layer-topping marine inversion, inversion-penetrating terrain, synoptic scale wind and pressure fields, nighttime drainage flows, and daytime/nighttime wind reversals produced by diurnal radiative cycles.

The smaller borderline meso-gamma/meso-beta scale eddies photographed and investigated in the current research appear to be mechanically-driven transient features (see the discussion by Hubert and Kruger 1962), lasting several hours. Such order-10 km eddies are important as they have been hypothesized to play a role in mixing at the coastal margin and have been implicated in cross-inversion fluxes of ozone and momentum (Lester 1985). Furthermore, they could lead to unexpected wind shifts for sailors or pilots, and anecdotal reports suggest an environment of strong aircraft turbulence in the lee of islands that produce similar eddies (Bob Baxter, Paul Ruscher, personal communicatons). Indeed, strong turbulence in the lee of the Hawaiian island of Kauai was documented as a cause of the breakup and crash of NASA’s ultralight unmanned aerial vehicle Helios (Porter et al, 2007). While the satellite imagery indicates that their appearance and scale are similar to those found in Von Karman vortex streets (e.g., Young and Zawislak 2006), the eddies presented here occurred individually and not as part of a series, although there is evidence that the Grover Beach eddy actually was the second one to form in the area that morning.

Although radiometric imagery of such features from weather satellites is common, the cases presented in this paper are notable in that *photographic* documentation of atmospheric eddies at this scale has been lacking in the meteorological literature. To our knowledge, these are the first close-up photographs of marine stratocumulus eddies, taken from an airplane, to appear in publication. Furthermore, because of their small scale, such eddies often pass between observation stations or occur within island wakes over the open ocean making them difficult to measure directly. This has left some basic questions not completely resolved, such as the nature of the cloud-free eye, and whether their circulations are only an inversion-level feature (as indicated by their cloud-free eye) or if they penetrate through the MABL all the way to the surface (Young and Zavislak 2006).

In the current case, satellite observations reveal that the eddy photographed near Grover Beach originally emerged offshore just south of Pt. Buchon moving toward the southwest, and passed directly through the three-station monitoring network run by Pacific Gas and Electric (PG&E) Company in support of their Diablo Canyon Nuclear Power Plant operations (Thuillier [1987] described PG&E's wind measurement efforts for emergency response in this complex terrain region). The eddy's path then turned toward the east, passing by and influencing wind directions at a surface observing station run by California Polytechnic State University (Cal Poly) on the Cal Poly Center for

Coastal Marine Sciences Pier. Finally, after being photographed just offshore by the pilot, the eddy moved inland over Grover Beach, this time through a coastal wind monitoring network operated by the San Luis Obispo County Air Pollution Control District (SLOAPCD). During its lifetime on satellite imagery, the eddy was close enough to influence surface wind measurements at three different observing stations. Furthermore it moved directly over PG&E's 76 m instrumented tower, allowing for direct observations of the surface and low level circulations and temperature structure, and subsequently directly over SLOAPCD's Grover Beach wind monitoring station, causing a nearly 180 degree wind direction reversal over a period of one minute. Note that without the special high resolution non-synoptic data obtained from PG&E, SLOAPCD, and Cal Poly for this study, it would not have been possible to document meteorological details of the eddy feature's passage through the area, as the only METAR in proximity is from San Luis Obispo, and it was unaffected by the circulation.

Given the relative frequency of mechanical eddies in satellite imagery, we speculate that pilots on the U.S. West Coast must see them periodically, but the current examples seem to be one of the few times that actual photographs have come to light in a scientific context. Since we received these images, a similar photograph from Sept. 2, 1993 also has come to our attention (Bill Brick, personal communication, Fig. 3). It was observed in the Santa Barbara channel, viewing approximately southward. Based on the description by Wilczak et al. (1991), it may be an example of a midchannel eddy (see also Kessler and Douglas 1991), or it may have been produced by Santa Cruz Island, similar to the July 16 2006 eddy.

The purpose of this paper is to present these unique photographic images of eddies near Grover Beach and Santa Cruz Island, to document their physical and dynamical characteristics, and to advance a hypothesis from the theoretical literature to explain their formation. It is intended that they will serve as a benchmark for verification and corroboration of numerical model simulations and studies on predictability of small-scale coastal effects, particularly where cross-inversion transport and mixing are important. This paper also demonstrates the value of high resolution coastal monitoring sites for detailed understanding of coastal processes. Confirmation of the photographed cloud features is provided in the form of corresponding satellite imagery, allowing nearly the complete eddy life cycles to be examined. Soundings, surface, and tower data will demonstrate that both circulations occurred with very strong temperature inversions above a relatively shallow MABL. Additionally, evidence of cross-inversion mixing will be presented from time series of winds and temperature as the Grover Beach eddy passed directly over the PG&E instrument tower. Finally, while the data presented do not permit an unambiguous conclusion on the formation mechanism of these eddies, it will be shown that the morphology and evolution of both is consistent with the hypothesis proposed by Smolarkiewicz and Rotunno (1989, hereafter referred to as SR1989): that is, tilting of "backward rolling" (negative) baroclinically generated horizontal vorticity into the vertical by vertical velocity differences between strong downslope flow directly in the lee of inversion-penetrating terrain and the weak or non-existent vertical motions on its periphery.

2. Eddy photographs and meteorological environment

a. Santa Cruz Island Eddy

The synoptic situation on July 16, 2006 included an inverted thermal trough in the interior of California extending northward from a climatologically typical thermal low over the California/Arizona border. The resulting onshore pressure gradient resulted in a northwesterly flow over the ocean west of most of California including over the westernmost Channel Island (San Miguel). However, a weak low pressure center, possibly a Catalina eddy circulation, was analyzed on the NCEP North American surface analyses for 06 and 09 UTC just north-northwest of Santa Cruz Island (not shown). This resulted in southeasterly surface flow in the near-shore environment and over Santa Cruz Island for a period of several hours during which the Santa Cruz Island eddy formed. At 500 hPa, southern California was under the influence of a west-east oriented ridge of high pressure centered north and east of the area, and helping to create easterly flow above 700 hPa and a strong temperature inversion just above the MABL.

The San Diego sounding (KNKX, Fig. 4) from 1200 UTC (Vandenberg, which is considerably closer, was unavailable) showed a strong inversion, with the MABL temperature at the inversion base of 20.6 ^{o}C at 293 m MSL (977 hPa), rising nearly 10 Celsius degrees over a vertical distance of about 500 m to 30.4 ^{o}C at 795 m MSL (925 hPa). The 1200 UTC Oakland sounding (KOAK, not shown) also showed a temperature inversion increase of 13 Celsius degrees from the surface (elevation 3 m MSL) to 613 m. The terrain in the eastern part of Santa Cruz Island rises to a peak elevation of roughly 550 m. In the context of previous studies that have shown mesoscale spatial variations of inversion height of hundreds of meters over land in the San Francisco Bay Area (Lester 1985), Los Angeles (Edinger 1959), over the ocean west of the California coast (Bridger et al. 1993) and near the Channel Islands (Eddington *et al*.1992), it is impossible to say with certainty what the MABL depth and inversion height was near the peak. Nevertheless, if we assume that the sounding environment near Santa Cruz Island was somewhere between the values at KOAK to the north and KNKX to the south, then we can conclude that the eastern peak of the island, at an elevation of 550 m, penetrates the base of the inversion, but may not extend to its top. Young and Zawislak (2006) note that island wake vortex streets typically occur downwind of steep islands that penetrate the inversion. Southerly winds through the depth of the temperature inversion (indicated by the KNXK RAOB) flowed over and around Santa Cruz Island, producing the photographed eddy on the north side of the island near its eastern periphery.

This first eddy photograph (Fig. 1) was taken at approximately 11:26 PDT (18:26 UTC) looking toward Santa Cruz Island to the west southwest. GOES Satellite imagery corroborates the existence of this eddy in the context of the larger-scale flow field. It also provides the ability to track the evolution and life-cycle of the eddy over the course of several hours, and to accurately estimate its dimensions at the satellite time most closely corresponding to the photograph, and other times as well. The satellite data were obtained from the NOAA (National Oceanic and Atmospheric Administration) Comprehensive Large Array-data Stewardship System (CLASS), remapped to a local perspective using McIDAS (Man computer Interactive Data Access System), then displayed and analyzed using GARP (GEMPAK [GEneral Meteorology PAckage] Analysis and Rendering Program). It should be noted that resolution limitations of the satellite imagery preclude fine scale analysis of structures that are clearly evident in the photographs.

In the sequence of visible satellite images covering the day of the photograph (Fig. 5), the corresponding image from 18:30 UTC is a close match in terms of cloud feature morphology. Several of the same features can be seen in both the satellite image and the photograph (Fig. 1), including the tongue of clouds extending from the tip of Santa Cruz Island toward the eddy, striations in the stratocumulus clouds on the northwest side of the eddy, and the cloud-free "eye."

Analysis of the 18:30 UTC satellite image using GARP indicates a circulation width of 9-10 km, length of 25 km, and cloud-free eye of 3 km; thus dimensions of this eddy near Santa Cruz Island straddle the line between the meso-gamma (2-20 km) and meso-beta (20-200 km) scales.

In the absence of direct in-situ observations or a detailed model simulation, conclusions on the formation mechanism of the Santa Cruz Island eddy must remain speculative. The following description and hypothesis are based on the satellite evidence and its consistency with previous theoretical results. The sequence of satellite images suggests that the dry air comprising the cloud-free eye of the eddy was wrapped laterally into the circulation from clear descending air near the north slope of the high terrain on Santa Cruz Island. This occurred near the eastern periphery of the island, consistent with SR1989's numerical simulation of vortices in low Froude number (i.e., very stable) flow past inversion-penetrating terrain. Calculation of Froude numbers using the San Diego sounding indicated a vertical distribution of values within the inversion ranging from 0.29 to 0.45, close to the "low Froude number" conditions investigated by SR1989, but transcritical conditions ($Fr \sim 1$) in the surface layer and above the temperature inversion. The apparent mechanism of vorticity production for this case may be synthesized from

SR1989, and theoretical results from Rotunno and Smolarkiewicz (1991), Rotunno and Smolarkiewicz (1995), Schär and Durran (1997), Rotunno et al. (1999), Epifanio and Durran (2002), and Epifanio and Rotunno (2005), and has also been invoked to explain real-world eddies like the Denver Cyclone (Crook et al. 1990) and the Santa Cruz eddy (Archer and Jacobson 2005). Based on these studies, we hypothesize that a favorable combination of strong static stability and ambient flow within the inversion layer air passing over the island top is accelerated downward in the lee of the island (*e.g.* Durran 2003). This produces a two-fold effect: (1) "backward rolling" (negative) baroclinically generated horizontal vorticity due to sloping isentropes, and (2) strong subsidence to the north of the high terrain side-by-side with non-vertically moving air over the open ocean, that is, differential vertical motion, initiating a tilting process wherein the "backward rolling" (negative) horizontal vortex tubes are bent downward into a vertical orientation. The strong sinking directly downwind of the high terrain brings down unsaturated air from above the marine layer, which also moves laterally into the cloud area, then becomes encircled in the eddy by the saturated air at the top of the MABL, forming the cloud-free eye. Section 2b.3 will present evidence from in-situ observations for this hypothesized formation mechanism in conjunction with the Grover Beach eddy.

Vorticity *within* the MABL flow below the inversion may also be contributed by the blocking effect of the island on its cool, dense air which cannot flow over the obstacle. This effect causes a deepening of the MABL on the upwind (south) side and a lowering of the inversion on the lee side, allowing for deeper penetration toward the surface by the warm, inversion layer air, and possibly reverse (northerly) MABL flow back toward the island on its lee side, similar to that following a retracting piston as described by Epifanio and Rotunno (2005). Within the overall southeasterly flow impinging on the island, this potential flow reversal on the lee (north) side of the island results in cyclonic vorticity generation within the MABL at the eastern periphery of the island.

A comment can be added here. The synoptic conditions on this day produced visible satellite imagery rich with low-level cloud phenomena. In fact, three eddies in the marine stratocumulus similar to the one later photographed near Grover Beach on September 12 also occurred in that area on the day of the Santa Cruz Island eddy photograph (July 16). Two can be seen in satellite animations (not shown) to rotate around each other south of Pt. San Luis. Additionally, a dramatic westward-propagating gravity wave train is evident in the marine stratocumulus clouds to the south of Santa Cruz Island, initiated by climatologically unusual thunderstorm activity reported in the 11 and 12 UTC San Diego METARs. Given the strong inversion and stability just above the MABL, conditions conducive for mechanical eddy formation also are conducive for pronounced gravity waves at the top of the MABL. Burk and Thompson (2004) have described a relationship between "shock-like" wave features and eddy formation in trans-critical flow (Froude number ~ 1).

b. Grover Beach Eddy

1) SYNOPTIC CONDITIONS

Synoptic scale weather conditions at the surface at 12 UTC on September 12, 2006, were characterized by an inverted thermal trough over the Central Valley of California. However, surface stations in the vicinity of San Luis Obispo indicate a weakly offshore pressure gradient in that region. The prevailing air flow just offshore along the coast as indicated by buoy stations was northwesterly around 5 m s^{-1} (10 kts). Several stations in the vicinity of the south central California coast were reporting fog or mist. At 500 hPa there was a high pressure area centered in northeastern Nevada, and a low centered over the California/Arizona/Mexico border. These two features combined to make lower tropospheric flow above the boundary layer easterly over the central to southern California coast.

The marine layer in the central and southern California coastal region was very shallow. For example, the Oakland sounding (not shown) indicated a surface-based inversion with a surface temperature at 3 m of 14.4 ^{o}C, versus a temperature of 19.4 ^{o}C at 122 m. The inversion top had a temperature of 27.4^{o}C at 805 m and 925 hPa. The San Diego sounding (not shown) indicated an inversion base of 17.2^{o}C at 251 m and 983 hPa with an inversion top of 26.4^{o}C at 709 m and 933 hPa. It would be preferable to use the sounding from the much-closer Vandenberg RAOB site, but crucial data were missing from its lower levels. Nevertheless, easterly to northeasterly flow aloft (seen most clearly in steady northeast winds at PG&E's Davis Peak station at an elevation of 550 m (1800 feet) and the very shallow depth of the MABL combine with the coastal terrain to limit inland penetration of the marine stratocumulus. Satellite imagery indicate that it is widespread over the ocean, but confined to the immediate coastal region over land. These weather characteristics are common during September in coastal California, indicative of marginal Santa Ana conditions that often prevail at this time of year.

2) SPECIAL METEOROLOGICAL DATA SOURCES

Three data sources provide direct evidence that the Grover Beach eddy's circulation extends down from cloud level (as seen in the photograph and satellite imagery) through the MABL all the way to the surface during most of its lifetime. The first was a three-station network operated by PG&E in support of their Diablo Canyon nuclear power plant. These stations consist of a 10 m tower located at Pt. Buchon at an elevation of 12.2 m (40 feet), a 20 m tower on Davis Peak in the San Luis Range at an elevation of 549 m (1800 feet), and their "Primary Meteorological" site, a 76 m tower at the plant itself (hereafter referred to as the "meteorological tower.") at 32 m (105 feet) MSL. The tower measures winds at 10 m and 76 m AGL, and temperature at 10 m, 46 m, and 76 m AGL. Pressure and humidity are not measured. Data from these stations were available every 15 minutes. The second data source is from the meteorological station at the Cal Poly Center for Coastal Marine Sciences Pier. This station contains a full suite of meteorological measurements on a four meter tower, archiving data every two minutes. The third data set comes from wind monitoring instruments operated by the San Luis Obispo County Air Pollution Control District (SLOAPCD), collecting observations every minute.

It should be noted that at the scales being examined in this paper, distances of less than a few kilometers and time periods of a few minutes become important for matching wind observations to satellite features. For example, at a speed of 3 m s^{-1} the eddy can move nearly 2.7 km, roughly the diameter of the cloud-free eye, in 15 minutes. Therefore, special care was taken to match images as closely as possible with the appropriate observation time. This involved calculating the time for the GOES-West Imager radiometer to scan to the latitude of the Diablo Canyon area, then determining the closest observations to that time for each of the three data sources, that is, the 15-minute PG&E data, the 2-minute CalPoly data, and the 1-minute SLOAPCD data. There can be a 1-4 minute lag time between the beginning of the GOES-West scan, and the time it takes to reach the latitude of the Diablo Canyon area, depending on which sector it is scanning.

3) GROVER BEACH EDDY DESCRIPTION AND ANALYSIS

The Grover Beach eddy was photographed at approximately 11:28 PDT (18:28 UTC) looking toward the west southwest (Fig. 2). Again, visible satellite imagery (Fig. 6) corroborates the existence of this flow feature and allows us to track the eddy's life cycle and the dimensions of its circulation. Satellite imagery and data from Davis Peak demonstrate that the terrain that produced the feature penetrated through the MABL into the inversion layer. The 1830 UTC satellite image (sixth panel in Fig. 6) is the time closest to the photograph time. Estimates made using GARP indicate that the eddy had a width of 9 km, was 17 km in length, and contained a cloud-free eye of 2.5-3 km at the time the photograph was taken. The stratocumulus field was much more extensive for this case than in the Santa Cruz Island case, clearly delineating the path of the eddy after formation around dawn.

The terrain that generated the eddy and locations of the relevant meteorological sites are shown on a relief map in Fig. 7. Directly north northwest of San Luis Bay is the San Luis Range (also known locally as the Irish Hills) with the higher ridges extending to between 450 to 550 m (1500-1800 feet) MSL. The Los Osos Valley containing San Luis Obispo can be found to the northeast. The satellite imagery in Fig. 6 includes wind and temperature observations superimposed using Unidata's Integrated Data Viewer (IDV). These images, selected from a more extensive satellite animation, indicate that the eddy originally emerged off the high terrain of the San Luis Range between 1400 and 1530

UTC just south of Pt. Buchon moving toward the southwest, parallel to the inversion-layer flow. The eddy becomes apparent in the marine stratocumulus as sunrise occurs. The initial eddy movement is consistent with the inversion-layer flow field as indicated by the steady northeast winds from the Davis Peak site, and likely downslope air movement in the lee of the ruggedly steep terrain of the coastal face of the San Luis Range (see Fig. 8)

As the sun comes up and the eddy first becomes apparent in the GOES-West imagery from 1430 to 1500 UTC, a strand of clouds begins to encircle the dry air that most likely subsided in a downslope mountain wave-like flow in the lee of the San Luis Range. Again it appears to be a combination of horizontal and vertical transport of unsaturated air from above the inversion base that produces the cloud-free eye. It is worthwhile to emphasize the steady northeasterly cross-ridge wind direction at Davis Peak. The strongest winds of the day of 6.2-6.5 m s^{-1}, a possible precursor of mountain wave activity, were recorded at 1415-1430 UTC at this station, just prior to the apparent eddy formation. This momentum may have mixed downward to the surface during the eddy formation process as will be seen in the wind time series showing stronger winds on the back side of the eddy during its passage over the meteorological tower. Evidence will be presented in this section that the inversion-layer air was indeed mixed down to the surface near the Diablo Canyon nuclear power plant.

When first evident on the satellite imagery as it emerges from the coastline, the cloud-free eye is 6-7 km in diameter, but shrinks to 2-3 km as it turns from moving southwestward to moving toward the east. The shrinkage of the eye is similar to that of von Karman vortices seen downwind of islands (Young and Zawislak 2006), suggesting a non-steady state boundary layer flow characterized by pressure gradient force, centrifugal force, and friction. It is interesting to note some features seen early in the eddy's life at 1600 UTC (Fig. 6): a band of clouds in the northwesterly flow piling up against the northwest face of the headland containing the San Luis Range, and a very similar band on the northwest flank of the cloud-free eye. Outside that is a dark band of apparently thin, less reflective clouds. These dark and light bands appear as the result of convergence between the southeasterly flow on the back side of the eddy, and the oppositional northwesterly flow over the ocean. The result is a smooth rim of thick, bright clouds surrounded by a dark area of thin clouds that at subsequent times is advected by the eddy circulation and encircles the eye. Thus the satellite imagery demonstrates the origins of the interweaved dark and light bands in the aerial photograph of the eddy (Fig. 2, corresponding to the 1830 UTC image in Fig. 6) spiraling in toward the eye and completely surrounding it.

Once the eddy emerges off the coastline its movement becomes more consistent with the westerly flow around the south side of the San Luis Range and Pt. San Luis. The change in direction suggests mixing of the inversion-layer air with the MABL air so the motion of the eddy, originally parallel to the inversion-layer flow, then becomes embedded within the boundary layer flow.

Surface and tower data (Fig. 6 and Fig. 9) corroborate Li et al.'s (2000) synthetic aperature radar results and Young and Zawislak's (2006) suggestion that the circulations of von Karman vortices observed in satellite imagery of island wakes can extend through the depth of the MABL to the surface. While the terrain feature here is not an island, it penetrates the temperature inversion and is completely surrounded by the MABL as an island would be. At least for the case of this shallow MABL, there is direct evidence that indeed the circulations evident in the cloud imagery were present in the surface wind field. Wind direction reversals of close to 180^{o} are seen at PG&E's meteorological tower as the eddy passes over the station (1445 and 1600UTC images from Fig. 6). Initial winds at 10 m before the eddy passage are northwesterly then shift to southeasterly after the cloud-free eye passes over the station. We estimate that the eddy is moving at approximately 1 m s^{-1} toward the southeast during this time period.

Winds at the 76 m level (Fig. 9) show a similar reversal, but it precedes that at 10 m by 15 minutes, presenting the intriguing possibility that the eddy has a forward slant from the surface to the upper level of the tower. This slant, along with the finite scanning period of the GOES satellite radiometer, may help to explain a slight apparent lag between the eddy position in the satellite images and the winds at the surface stations. Additionally, errors in the satellite image navigation and precision limitations in the map databases may cause map discrepancies of as much as two or more kilometers. Interestingly, the southeasterly "return flow" winds in opposition to the synoptic scale flow on the rear flank of the eddy were stronger at 10 m and 76 m (4.6 and 6.0 m s^{-1}, respectively) than either the winds directly before or after its passage, possibly indicating that the accelerated downslope winds of the mountain wave circulation are being converted to kinetic energy of the eddy.

As the eddy crossed San Luis Bay, winds at the Cal Poly pier swung from southerly (Fig. 6, 1700 UTC) to east southeasterly (1746 UTC). This is consistent with the eddy's cyclonic rotation as it passes to the south of the pier.

The 1830 UTC satellite image (Fig. 6) is closest in time to the Grover Beach eddy photograph (Fig. 2). At this time, winds from the Grover Beach station of the SLOAPCD network were reporting southerly winds, consistent with the cyclonic flow on the east side of the eddy. During the period between 1830 and 1911 UTC the GOES-West satellite was operated in rapid scan mode and images became available at 1840, 1846, 1852, 1900, and 1911 UTC during this period as a result. The cloud-free eye moves directly over the station as indicated by the 1846 UTC image (Fig. 6) and other subsequent images from 1852 and 1900 UTC (not shown). The wind from the Grover Beach station was reported as southeast at 2.2 m s^{-1} at 1846 UTC (note that these are the nominal times of the satellite image, and that according to the procedure outlined in Section 2b.2, the station data may actually be several minutes different depending on the actual time in the scan when the imager reached the Diablo Canyon area). By 1911 UTC (Fig. 6) the cloud-free eye had moved beyond the edge of the coastal stratocumulus and merged into the clear-air region to the east, while the reported wind at the Grover Beach station had shifted to a northwesterly direction at 3.6 m s^{-1}.

It is instructive to examine the time sequence of temperatures in comparison with the winds from the meteorological tower (Fig. 9). Prior to about 1445 UTC temperatures indicate that the entire tower is within the well-mixed MABL, with values at 10 m, 46 m, and 76 m hovering near 11^{o}C. As the eddy begins to pass over the tower, the winds are northwesterly and temperature at the 76 m level begins to rise, followed by a rise in temperature at 46 m, then at 10 m over a period of approximately an hour and a half. This sequence briefly establishes a surface-based temperature inversion during the duration of the eddy passage. This is followed by a drop in temperatures again initiating at the 76 m level followed by those at the 46 and 10 m levels 45 minutes later. The possibility of a forward slant in the eddy shape suggested by the wind fields would also explain this sequence of temperature changes. The increase in temperature at all three levels indicates that there is cross-inversion turbulent mixing of warm air from aloft down into the cool MABL in the lee of the rugged terrain of the San Luis Range. Goodman and Miller (1977) hypothesized cross-inversion mixing in the *horizontal* direction in the presence of sloped inversions based on measurements from the 299 m Sutro Tower atop 277 m Mt. Sutro, and tracer experiments of the inversion in the San Francisco Bay Area. The sequence of temperature measurements here imply a strongly sloped inversion and support Lester's (1985) implication of order-10 km scale eddies in cross-inversion mixing.

4) FROUDE NUMBER AND POSSIBLE EDDY FORMATION MECHANISM

SR1989 used idealized model simulations in order to understand wake vortex formation in the lee of the Hawaiian Islands. Their results suggest the importance of Froude Number (Fr) in the range 0.5-0.1 in eddy formation. Fr is a dimensionless ratio comparing inertial with buoyancy forces in the flow field, and values considerably less than 1 usually mean that the atmosphere is very stable. Here the Oakland and San Diego soundings and wind speed at Davis Peak are used to estimate a Fr based on the formulation employed by SR1989:

$$Fr = \frac{U}{N \cdot h} \qquad (1)$$

where U is the speed of the flow approaching a mountain, h is a characteristic mountain height (taken as 550 m, the height of Davis Peak), and N is the Brunt-Vaisala frequency.

This form of Fr applies for the continuously stratified real atmospheric environment presented in this case. N is given by

$$N = \sqrt{\frac{g}{\theta_v} \cdot \frac{\partial \theta_v}{\partial z}} \qquad (2)$$

(e.g., Young and Zawislak 2006) where in practice we averaged the virtual potential temperature, θ_v between two discrete levels of the sounding, and the vertical derivative of virtual potential temperature was approximated using the values at those discrete levels. g is the acceleration of gravity.

As described in Section 2b.3, it appears that the eddy was initiated in the inversion-layer northeasterly flow over the San Luis Range, and therefore Fr was estimated for mountain-top level based on the 12UTC Oakland and San Diego soundings, since Vandenberg was missing data from the relevant lower levels. As noted in Section 2a, there can be considerable variability in inversions over coastal California, and the distances between the Diablo Canyon area and the Oakland or San Diego sounding sites are approximately 320 and 430 km, respectively. Additionally, N varies vertically in a continuously stratified atmosphere. Therefore, N was calculated individually from both the Oakland and San Diego soundings for their layers encompassing the height of Davis Peak, representative of the tops of the San Luis Range. Fr for each was allowed to vary in time based only on variations in U, the speed of the flow impinging at mountain top level as indicated by wind speed from the Davis Peak monitoring site. The Fr values from each sounding at each time then were averaged together. Results indicate Fr values varying within the 0.3-0.5 range, consistent with SR1989.

Wind speed observations and the Fr estimates at different times prior to and at the beginning of eddy formation are shown in Table 1. SR1989 idealized model simulations indicate that atmospheric lee vortices at a Fr of 0.3 form by tilting of baroclinically generated horizontal vorticity. While the current data set is not detailed enough to unambiguously confirm their hypothesis in this case, behavior and physical characteristics of the Grover Beach eddy are consistent with such a mechanism. The meteorological tower data provide direct evidence meeting SR1989's suggested observational test (p. 1164) that such vortices should have a warm core (see also Schär and Durran 1997). This is seen in the previously-noted temperature increases at all three tower levels during eddy passage (Fig. 9). This warm core requires an injection of inversion-layer air into the MABL, which under SR1989's mechanism is provided in a mountain wave-like sinking in the lee of the San Luis Range that also provides the dry air for the cloud-free eye, and may also be facilitated by the blocking effect of the terrain on the MABL and consequent lowering of its top downwind of the terrain (Epifanio and Rotunno 2005).

Again, based on a synthesis of results from theoretical studies of eddy formation dealing with baroclinic generation of horizontal vorticity and subsequent tilting to a vertical axis (SR1989; Rotunno and Smolarkiewicz 1991; Rotunno and Smolarkiewicz 1995; Rotunno et al. 1999; Schär and Durran 1997; Crook et al. 1990; Epifanio and Durran 2002, and Epifanio and Rotunno 2005), we can describe the possible formation mechanism of the Grover Beach eddy: a favorable combination of strong static stability and ambient northeasterly flow within the inversion layer air near mountain-top level creates a downslope wind acceleration on the lee (southwest) side of the mountain peak (in our case the raised terrain of the San Luis Range) as in Rotunno and Smolarkiewicz's (1995) Figure 3 reproduced here as Figure 10. Negative horizontal vorticity (i.e. rotation around a horizontal axis) is generated here baroclinically along sloping isentropic surfaces, the result being a "backward" rolling motion and overturning as the fast-moving surface level flow undercuts the slower flow above it. The finite width of the hills means that the maximum downward acceleration of the flow is directly in the lee of the highest terrain and decreases to negligible on either side beyond the flanks of the terrain. This results in differential downward vertical velocity tilting the backward rolling horizontal vortex tube downward into a vertical orientation. Figure 11 shows a schematic view of this process (based on the concept illustrated in Figure 3c of Rotunno and Smolarkiewicz 1991) superimposed on an aerial photograph of the region between the Diablo Canyon nuclear power plant and Pt. Buchon. Looking upwind toward the oncoming flow, the maximum downward vertical velocity in the lee of the centerline of the highest terrain produces a counterclockwise or cyclonically-rotating vortex to its left (Rotunno et al. 1999; Rotunno and Smolarkiewicz 1991). This mechanism would explain why the maximum temperatures seen during the eddy passage in Figure 9 occur not at the center of the wind reversal, but within the southeasterly winds on the rear flank of the eddy during this early period in its life-cycle. The tilting mechanism requires greater downward vertical motion to the right of the eddy (looking upwind) during its formation, therefore this should be a region containing a higher proportion of warm inversion air, at least in the incipient stages of the eddy. This air moves into the rear of the eddy with its cyclonic circulation. SR1989's mechanism would appear to explain the initial eddy motion paralleling the inversion-layer northeasterly flow, but subsequently moving along with the MABL flow rounding San Luis point toward the east.

As with the Santa Cruz Island case, it seems likely that the blocking effect (again, see Epifanio and Rotunno 2005) of the high terrain on the cool, dense, northerly air flow of the MABL contributes to cyclonic vorticity formation *within* that layer phasing with that produced within the inversion. Again, the blocking effect contributes to the lowering of the MABL top in the lee of the terrain, allowing the inversion layer air to penetrate more easily to the surface.

Some final points are in order. Casual examination of visible satellite images in the seven years since the eddy images were sent to us have revealed that it is not unusual for eddies to come spinning off the raised terrain of the San Luis Range. Its prominence as terrain that protrudes westward into the marine environment, while frequently penetrating the inversion above, creates conditions that are likely to produce eddies in ways similar to large islands like Santa Cruz and Catalina, and thus may often produce conditions for cross-inversion mixing and transport, a potentially important phenomenon if pollution or toxins are present.

SR1989's eddy formation mechanism explains another observation we have noticed in satellite imagery over the years (and that was seen in the Santa Cruz Island satellite feature): when eddies form in the lee of inversion-penetrating high terrain, the dry air appears to move laterally into the eddy before the stratocumulus clouds wrap around the rear flank closing off the cloud-free eye. This would be due to the greatest downward vertical velocity not being in the center of the cyclonic eddy, but being to the right of it looking upwind during its formation stage, consistent with the vorticity tilting that produces the eddy.

3. Summary and conclusions

Unique aerial photographs of cyclonic eddies in the marine stratocumulus taken by a commercial pilot off the California coast have been presented. The eddies were similar in scale and appearance to Von Karman vortices seen in high resolution satellite imagery and described in the literature. Each had a cloud-free eye, and occurred under strong inversion conditions with a shallow MABL. While satellite imagery of such features has previously been presented, to our knowledge, these are the first photographic images of such features, taken from an airplane, to appear in publication.

The eddies occurred in the lee of inversion-penetrating high terrain of Santa Cruz Island and the San Luis Range, a headland near San Luis Obispo. The latter eddy then drifted toward Grover Beach where it was photographed by the pilot.

GOES satellite imagery, along with non-synoptic meteorological observing sites in the case of the Grover Beach eddy, shed light on the formation and evolution of these eddies. A three-level 76 m instrumented tower, run by PG&E for monitoring at their Diablo Canyon nuclear power plant, was found to be directly in the path of the Grover Beach eddy as was a surface wind monitoring site run by the SLOAPCD. These instruments showed nearly 180 degree reversals coincident with the passage of the cloud-free eye of the Grover Beach eddy, demonstrating that this eddy was not just an inversion-level cloud feature, but penetrated the MABL to the surface.

Data from the Diablo Canyon meteorological tower are consistent with the eddy formation mechanism suggested by SR1989 of baroclinic vorticity generation from sloped isentropes resulting in a "backward" rolling motion that then gets tilted into the vertical by the differential downward flow in the lee of the finite-width high terrain. Their suggestion of a warm core eddy is confirmed with temperature rises of up to $2C^{o}$ at all three tower levels, and the descent of the inversion to the surface with the passage of the eddy. This temperature rise represents an apparent injection of warmer and drier inversion-layer air, and cross-inversion mixing downward into the MABL, resulting in the cloud-free eye seen in the images.

The eddy appears to have been initiated in the inversion layer flow, but then becomes embedded within the well-mixed MABL flow. At the beginning of its life-cycle, the Grover Beach eddy appeared to be moving with the inversion-layer northeasterly flow evident at the Davis Peak site. Subsequent to the eddy formation and the presumed injection of warm, dry air into the MABL, the eddy turned and moved along with the boundary layer flow rounding Pt. San Luis and over Grover Beach.

The wind reversals at the meteorological tower appeared to slightly lag the satellite feature. Some of this lag may be accounted for by the delay of the GOES Imager instrument between the nominal image time and when the scanner reaches the latitude of the eddy (1-4 minutes) in combination with the 15 minute resolution of the PG&E data. Errors in satellite navigation may also have contributed. However, data from the 76 meter tower also suggest that the eddy was leaning forward, which could also account for some of the apparent lag. Wind reversals associated with the eddy passage at 76 m preceded those at 10 m by 15 minutes, and temperature rises and falls more than at the lower levels.

It has become clear from examination of visible satellite imagery of the Grover Beach area in the time since the eddy photographs first came to light that the high terrain of the San Luis Mountains generates similar eddies in the marine stratocumulus frequently. In fact, on the day of the *Santa Cruz Island* eddy photograph, at least three eddies also were generated near the San Luis Range, two of which can be seen in satellite imagery to rotate around each other in the San Luis Bay (not shown). A more complete understanding of eddy formation mechanisms in this area along with cross-inversion mixing processes and air transport mechanisms in and around the eddies will require very high resolution model simulations or a detailed field experiment.

Acknowledgments. This research became possible with much thanks to former Embry-Riddle Aeronautical University (ERAU) student and flight instructor, and current Skywest pilot Captain Peter Weiss, who originally sent us these unique eddy photographs, and "KB" who actually photographed the eddies. We gratefully acknowledge John Lindsey and Ed McCarthy of PG&E, Brian Zelenke of Cal Poly, and Gary Arcemont and Joel Craig of San Luis Obispo County Air Pollution Control District. All were instrumental in providing the available meteorological observations. The base map used in Figure 7 was obtained courtesy of the San Luis Obispo County Planning Department, Geographic Technology and Design Section. Pete Lester shared some difficult-to-find NSF reports. Bill Brick of the San Diego County Air Pollution Control District provided the additional eddy photograph of the midchannel eddy taken by Trudy Wood. ERAU Applied Meteorology system administrator Robert Haley gave us invaluable assistance in data processing and with some of the figures. We thank Paul Ruscher and Bob Baxter for sharing their personal knowledge and experiences. We appreciate the assistance of Dr. Mike Hickey and ERAU in providing funding for publication.

This research benefited tremendously from several government-sponsored programs and software packages: NOAA’s CLASS; the McIDAS, GARP, and IDV software packages provided by NSF’s Unidata program; and NCL (NCAR [National Center for Atmospheric Research] Command Language) provided by NSF’s NCAR.

References

Alpert, T., M. Tzidulko, and D. Iziksohn, 1999: A shallow, shortlived meso-β cyclone over the Gulf of Antalya, eastern Mediterranean. *Tellus*, **51A**, 249–262.

Archer, C. L., M. Z. Jacobson, and F. L. Ludwig, 2005: The Santa Cruz Eddy. Part I: Observations and statistics. *Mon. Wea. Rev.*, **133**, 767-782.

_____ and _____, 2005: The Santa Cruz Eddy. Part II: Mechanisms of formation. *Mon. Wea. Rev.*, **133**, 2387-2405.

Bosart, L. F., 1983: Analysis of a California Catalina eddy event. *Mon. Wea. Rev.*, **111**, 1619–1633.

Bridger, A. F. C., W. C. Brick, and P. F. Lester, 1993: The structure of the marine inversion layer off the central California coast: Mesoscale conditions. *Mon. Wea. Rev.*,**121**, 335–351.

Burk, S. D., and W. T. Thompson, 2004: Mesoscale eddy formation and shock features associated with a coastally trapped disturbance. *Mon. Wea. Rev.*, **132**, 2204-2223.

Chopra, K. P., and L. F. Hubert, 1965: Mesoscale eddies in wakes of islands. *J. Atmos. Sci.*, **22**, 652–657.

Crook, N. A., T. L. Clark, and M. W. Moncrieff, 1990: The Denver Cyclone. Part I: Generation in low Froude number flow. *J. Atmos. Sci*., **47**, 2725–2742.

Dorman, C. E. and C. D. Winant, 2000: The structure and variability of the marine atmosphere around the Santa Barbara channel. *Mon. Wea. Rev.*, **128**, 261–282

Douglas, S. G., and R. C. Kessler, 1991: Analysis of mesoscale airflow patterns in the south-central coast air basin during the SCCCAMP 1985 intensive measurement periods. J. *Appl. Meteor.*, **30**, 607–631.

Durran, D. L., 2003: Downslope winds. *Encyclopedia of Atmospheric Sciences.* J. R. Holton, J. A. Curry and J. A. Pyle, Eds., Elsevier, 644-650.

Eddington, L. W., J. J. O'Brien, and D. W. Stuart, 1992: Numerical simulation of topographically forced mesoscale variability in a well-mixed marine layer. *Mon. Wea. Rev.*, **120**, 2881–2896.

Edinger, J. G., 1959: Changes in the depth of the marine layer over the Los Angeles Basin. *J. Meteor.*, **3**, 219–226.

Epifanio, C. C., and D. R. Durran, 2002: Lee-vortex formation in free-slip stratified flow over ridges. Part II: Mechanisms of vorticity and PV formation in nonlinear viscous wakes. *J. Atmos. Sci.*, **59**, 1166–1181.

_____ and R. Rotunno, 2005: The dynamics of orographic wake formation in flows with upstream blocking. *J. Atmos. Sci.*, **62**, 3127–3150.

Etling, D., 1989: On atmospheric vortex streets in the wake of large islands. *Meteor. Atmos. Phys.*, **41**, 157–164.

Goodman, J. and A. Miller, 1977: Mass transport across a temperature inversion. *J. Geophys. Res.*, **82**, 3463-3471.

Hanna, S. R., D. G Strimaitus, J. S. Scire, G. E. Moore, and R. C. Kessler, 1991: Overview of results of analysis of data from the South-Central Coast Cooperative Aerometric Monitoring Program (SCCCAMP 1985). *J. Appl. Meteor.*, **30**, 511–533.

Hubert, L. F., and A. F. Krueger, 1962: Satellite pictures of mesoscale eddies. *Mon. Wea. Rev.*, **90**, 457–463.

Kessler, R. C., and S. G. Douglas, 1991: Numerical simulation of topographically forced mesoscale variability in a well-mixed marine layer. *J. Appl. Meteor.*, **30**, 633–651.

Lester, P. F., 1985: Studies of the marine inversion over the San Francisco Bay area. A summary of the work of Albert Miller, 1961–1978. *Bull. Amer. Meteor. Soc.*,**66**, 1396–1402.

Li, X., P. Clemente-Colon, W. G. Pichel, and P. W. Vachon, 2000: Atmospheric vortex streets on a RADARSAT SAR image. *Geophys. Res. Lett.*, **27**, 1655–1658.

Lyons, W. A., and T. Fujita, 1968: Mesoscale motions in oceanic stratus as revealed by satellite data. *Mon. Wea. Rev.*, **96**, 304–314.

Mass, C. F., and M. D. Albright, 1989: Origin of the Catalina eddy. *Mon. Wea. Rev.*, **117**, 2406–2436.

Parish, Thomas R., David A. Rahn, Dave Leon, 2013: Airborne Observations of a Catalina Eddy. *Mon. Wea. Rev.*, **141**, 3300–3313.

Porter, J. N., D. Stevens, K. Roe, S. Kono, D. Kress and E. Lau, 2007: Wind environment in the lee of Kauai Island, Hawaii during trade wind conditions: weather setting the the Helios mishap. *Bound.-Layer Meteor.* **123**, 463-480.

Orlanski, I., 1975: A rational subdivision of scales for atmospheric processes. *Bull. Amer. Meteor. Soc.*, **56**, 527-530.

Rosenthal, J., 1968: A Catalina Eddy. *Mon. Wea. Rev.*, **96**, 742-743.

Rotunno, R., and P. K. Smolarkiewicz, 1991: Further results on lee vortices in low-Froude-number flow. *J. Atmos. Sci.*, **48**, 2204–2211.

_____ and _____, 1995: Vorticity generation in the shallow-water equations as applied to hydraulic jumps. *J. Atmos. Sci.*, **52**, 320-330.

_____, V. Grubisic, and _____, 1999: Vorticity and potential vorticity in mountain wakes. *J. Atmos. Sci.*, **56**, 2796-2810.

Ruscher, P. H., and J. W. Deardorff, 1982: A numerical simulation of an atmospheric vortex street. *Tellus*, **34**, 555-566.

Schär, C., and D.R. Durran, 1997: Vortex formation and vortex shedding in continuously stratified flows past isolated topography. *J. Atmos. Sci.*, **54**, 534-554.

Smolarkiewicz, P. K., and R. Rotunno, 1989: Low Froude number flow past three-dimensional obstacles. Part I: Baroclinically generated lee vortices. *J. Atmos. Sci.*, **46,** 1154–1164.

Thompson, W. T., S. D. Burk, and J. Rosenthal, 1997: An investigation of the Catalina eddy. *Mon. Wea. Rev.*, **125**, 1135–1146.

Thomson, R. E., J. F. R. Gower, and N. W. Bowker, 1977: Vortex streets in the wake of the Aleutian Islands. *Mon. Wea. Rev.*, **105**, 873–884.

Thuillier, R. H., 1987: Real-time analysis of local wind patterns for application to nuclear-emergency response. *Bull. Amer. Meteor. Soc.*, **68**, 1111-1115.

Wakimoto, R. M., 1987: The Catalina eddy and its effect on pollution over southern California. *Mon. Wea. Rev.*, **115**, 837–855.

Wilczak, J. M., W. F. Dabberdt, and R. A. Kropfli, 1991: Observations and numerical-model simulations of the atmospheric boundary layer in the Santa Barbara coastal region. *J. Appl. Meteor.*, **30**, 652–673.

Young, G.S., and J. Zawislak, 2006: An observational study of vortex spacing in island wake vortex streets. *Mon. Wea. Rev.*, **134**, 2285-2294.

Table 1. Froude Number calculations from Equations (1) and (2) where the inversion layer wind from Davis Peak is U. The value in the table represents the average Fr from a mountain-top layer of both the Oakland (KOAK) and San Diego (KNKX) soundings.

Time	U (Davis Peak)	Froude Number (Avg. KOAK & KVBG)
1100	5.1	0.35
1115	4.7	0.32
1130	4.9	0.34
1145	5.1	0.35
1200	5.2	0.35
1215	5.1	0.35
1230	4.8	0.33
1245	4.8	0.33
1300	5.5	0.38
1315	5.1	0.36
1330	5.0	0.34
1345	4.9	0.33
1400	5.8	0.40
1415	6.2	0.43

1430	6.5	0.45
1445	6.0	0.41
1500	6.0	0.41

Figure 1. Aerial photograph of stratocumulus cloud vortex just north of Santa Cruz Island on July 16, 2006 at 11:26 PDT (18:26 UTC), viewing toward the southwest. (Photo by "KB" courtesy of Capt. Peter Weiss of SkyWest Airlines).

Figure 2. Aerial photograph of stratocumulus cloud vortex just offshore from Grover Beach, California, on September 12, 2006 at 11:28 PDT (18:28 UTC). (Photo by “KB” courtesy of Capt. Peter Weiss of SkyWest Airlines).

Figure 3. Aerial photograph of stratocumulus cloud vortex in the Santa Barbara Channel on September 2, 1993. (Photo by Trudy Wood courtesy of Bill Brick).

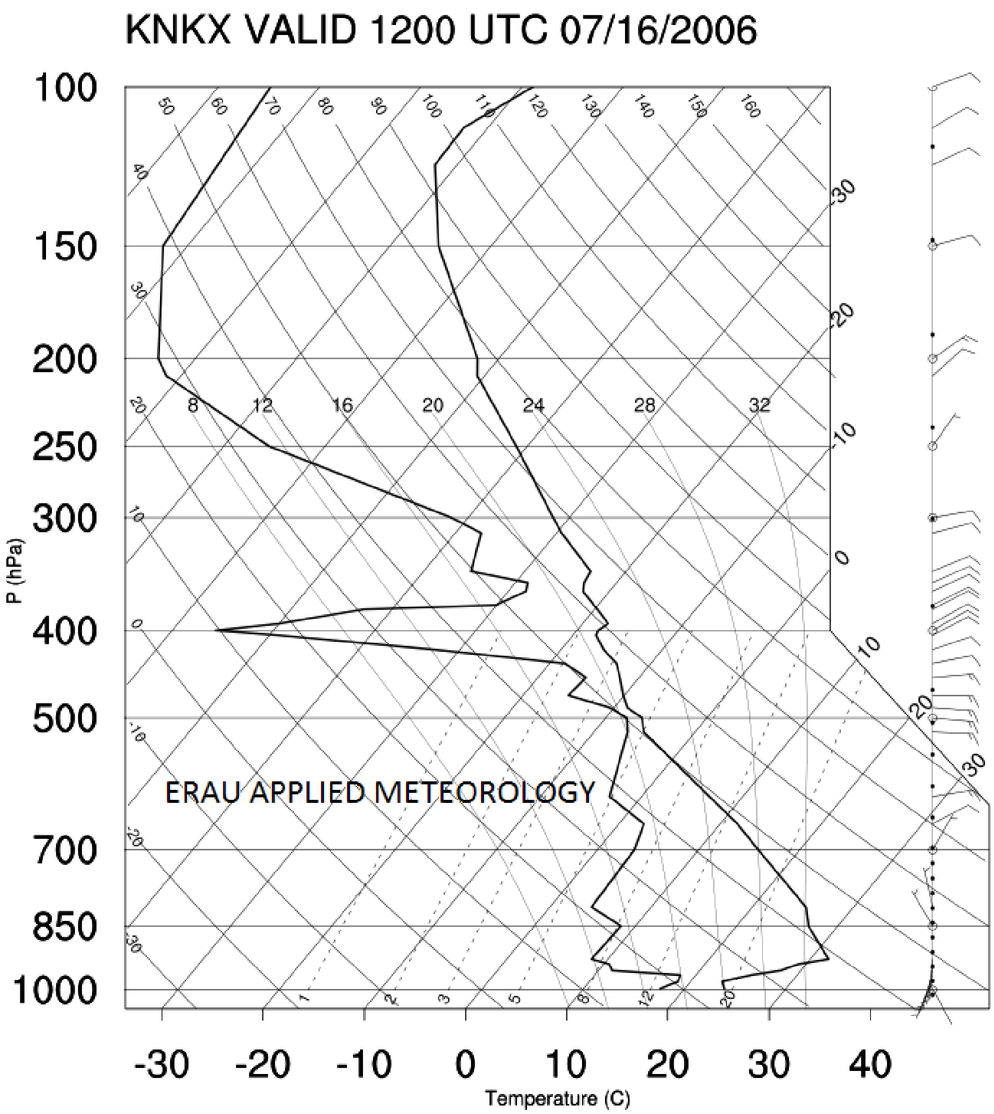

Figure 4. San Diego rawinsonde sounding from 12 UTC on July 16 2006 showing the strong low-level inversion with the temperature of the marine atmospheric boundary layer rising from 20.6^{o}C at 293 m MSL to 30.4^{o}C at 795 m MSL. The peak elevation of Santa Cruz Island is roughly 550 m.

Figure 5. GOES-West visible satellite images from 17:00 UTC to 18:30 UTC on July 16, 2006. In this sequence, dry, cloud-free air in the lee of Santa Cruz Island can be seen moving laterally into the circulation followed by a tongue of clouds wrapping around and closing off the "eye." The satellite image from 18:30 UTC shows the same cloud as

figure 1. Analysis of this cloud indicates the width to be 9-10 km, a length of 25 km, and a cloud-free eye of 3 km.

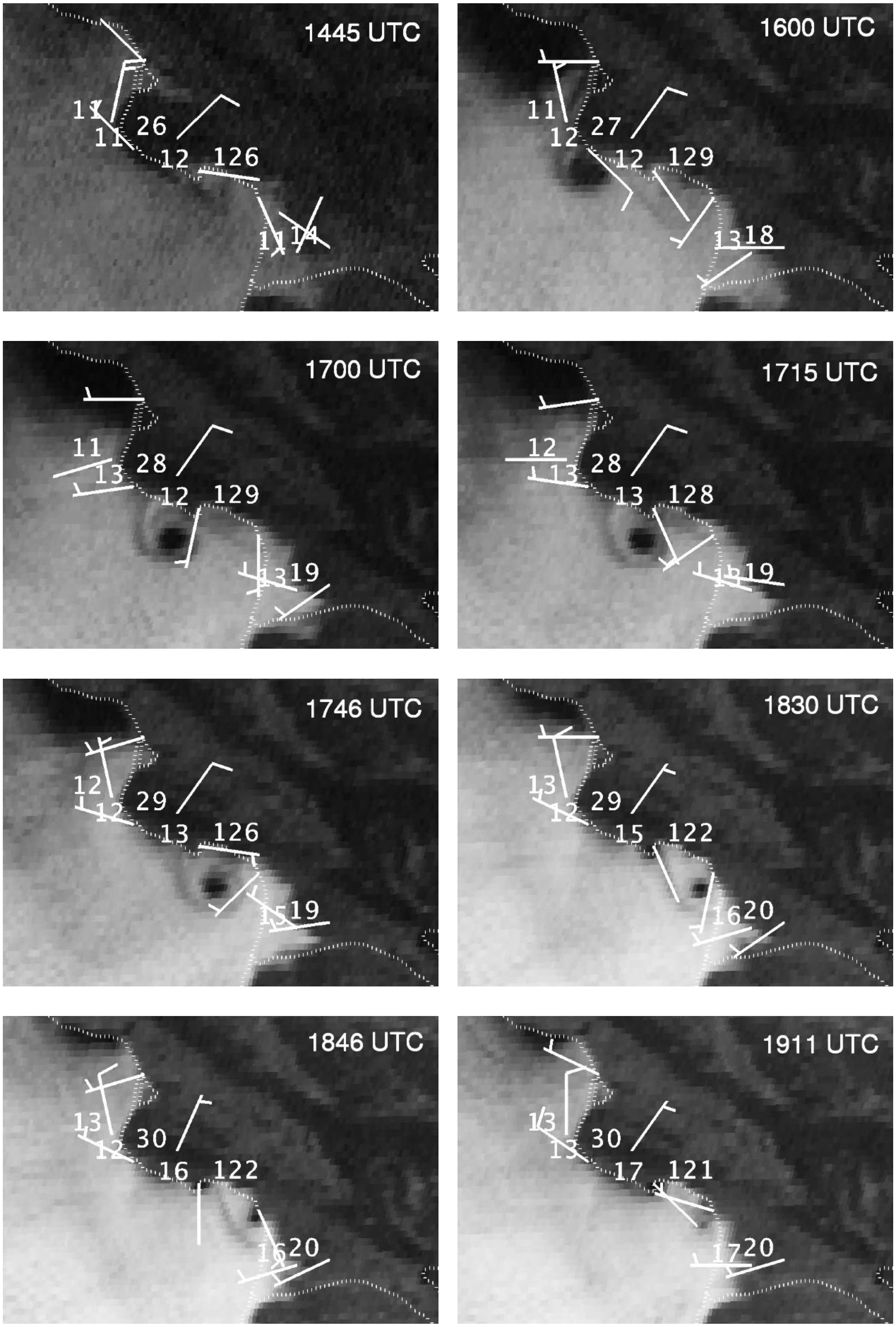
1445 UTC
26
12
126
11
14
1600 UTC
11
12
27
12
129
18
1700 UTC
11
13
28
12
129
19
1715 UTC
12
13
28
13
128
19
1746 UTC
12
12
29
13
126
19
1830 UTC
13
12
29
15
122
16
20
1846 UTC
13
12
30
16
122
20
1911 UTC
13
30
17
121
20

Figure 6. GOES-west images from 14:45 to 19:11 UTC on Sept. 12, 2006 showing the Grover Beach eddy. The satellite image at 1830 UTC shows the same cloud as figure 2. Analysis of the image shows shows a length of 17 km, width of 9 km, and cloud-free eye of 2.5-3 km. Half barbs represent wind speeds of approximately 2.5 ms^{-1}. Whole barbs represent wind speeds of approximately 5 ms^{-1}, and a shaft with no barb represents wind speeds of less than approximately 1.3 ms^{-1} but greater than 0.26 ms^{-1}. Circles depict wind speeds of less than approximately 0.26 ms^{-1}.

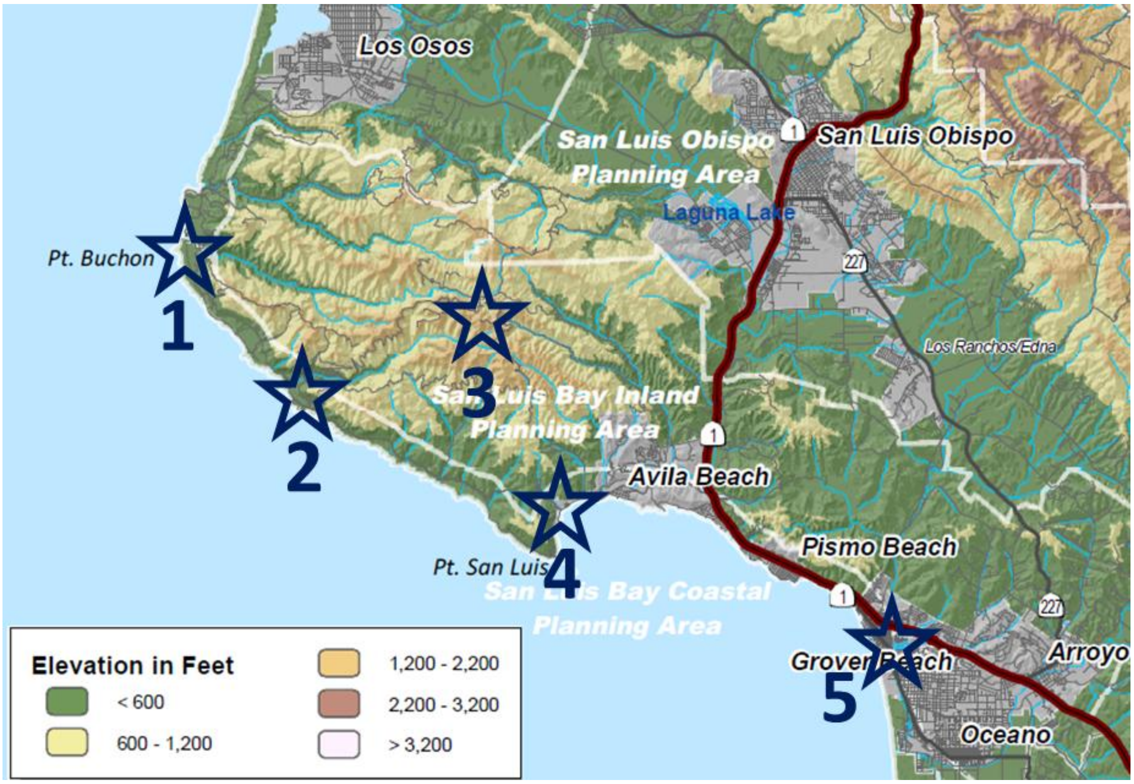

Figure 7. Terrain that produced the Grover Beach eddy, with the locations of relevant monitoring stations superimposed and numbered as follows: 1) Pt. Buchon 2) Diablo Canyon Nuclear Power Plant meteorological tower 3) Davis Peak 4) Cal Poly pier 5) SLOAPCD Grover Beach site. Just to the north northwest of San Luis Bay is the San Luis Range (also known locally as the Irish Hills) which has ridges extending to between 450 to 550 m (1500-1800 feet) MSL. (Base map courtesy of San Luis Obispo County Planning Department, Geographic Technology and Design Section).

Figure 8. Diablo Canyon nuclear power plant with the San Luis Range, the terrain that produced the Grover Beach eddy. Note the meteorology instrument tower in the top panel in front of the plant. (Photos courtesy of John Lindsey, PG&E).

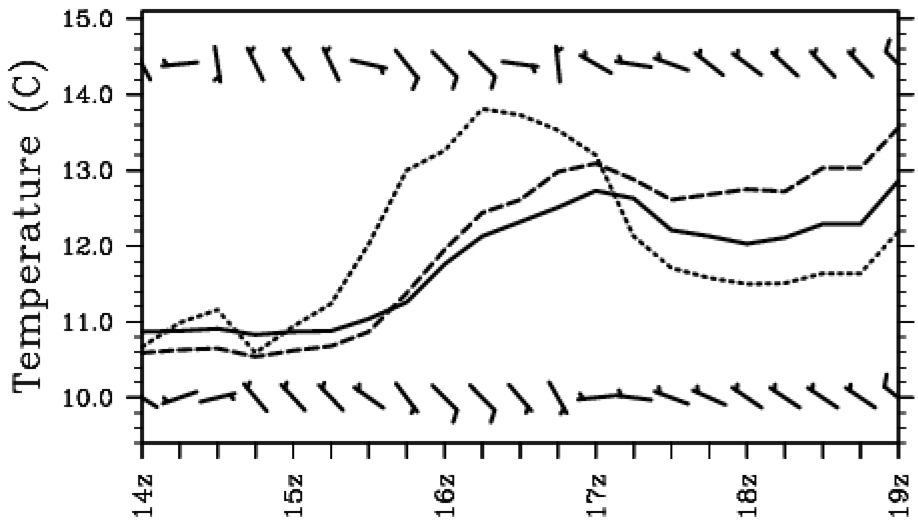

742 **Figure 9.** Temperature (^{o}C) time series (curves) from three levels, and wind time series

743 (barbs) from two levels collected by the instrumented tower at the Diablo Canyon nuclear

744 power plant, as the eddy passed over. The dotted curve is from 76 m, dashed curve is

745 from 46 m, and the solid curve is from 10 m above ground level (AGL). The top row of

746 winds is from 76 m and the bottom row is from 10 m AGL. Half barbs indicate

747 approximately 2.5 ms^{-1} and whole barbs approximately 5 ms^{-1}. Time is in UTC. Note

748 that the fastest winds during the period occur in the southeasterly flow of the eddy's rear

749 flank.

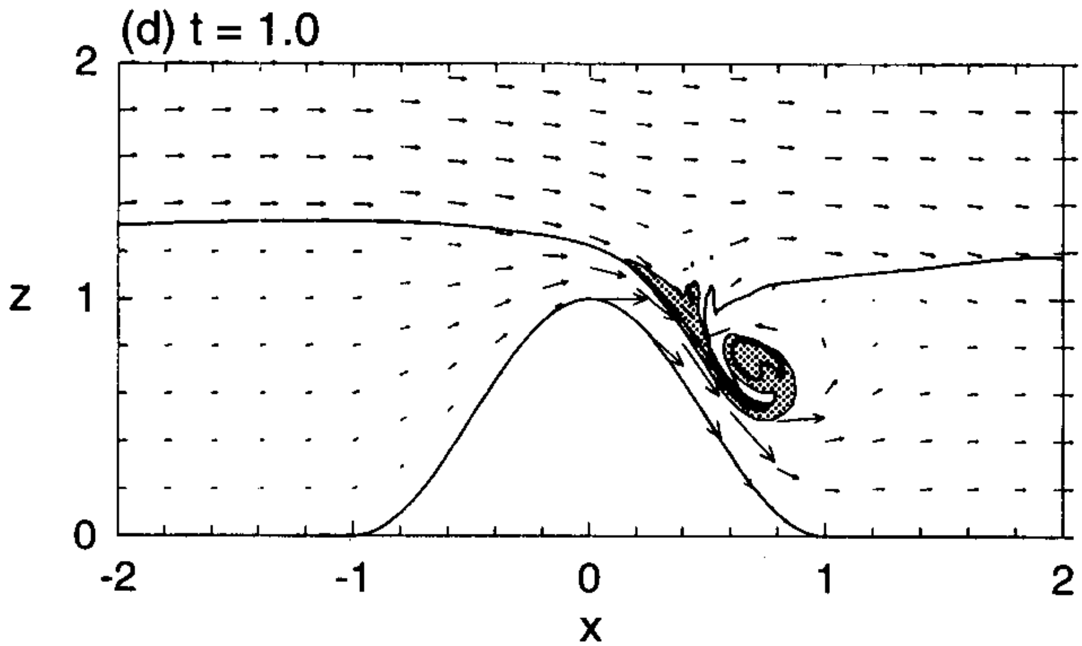

Figure 10. (from Rotunno and Smolarkiewicz 1995 Figure 3 d). Negative horizontal vorticity (i.e., rotation around a horizontal axis) generated baroclinically by flow along sloping isentropic surfaces, which results in a "backward" (with respect to the mean flow) rolling or overturning motion as the fast moving surface flow undercuts the slower flow above it.

Figure 11. Schematic depiction of the “backwards” rolling horizontal vortex tube being tilted downward into a vertical orientation by the differential vertical velocities between the weak or nonexistent downward motion on the periphery of the high terrain and the maximum downward motion at the terrain centerline (see Figure 3c in Rotunno and Smolarkiewicz 1991) . Viewing upwind against the flow as in this figure, this produces a cyclonically rotating vortex to the left of the centerline.